# UNITED STATES NAVAL ACADEMY

## DIVISION OF
## ENGINEERING AND WEAPONS

# A TECHNIQUE TO LOCATE DAMAGE IN A BEAM USING NON-RESONANT FREQUENCY RESPONSE VIBRATION DATA

**Colin P. Ratcliffe**

**TECHNICAL REPORT EW-07-97**
**JULY 1997**

## MECHANICAL ENGINEERING
## DEPARTMENT

Dr. Colin P. Ratcliffe
Mechanical Engineering Department
United States Naval Academy
590 Holloway Road
Annapolis, MD 21402-5002
(410) 293-6535
email: ratcliff@nadn.navy.mil

EW-07-97 July 1997

# A TECHNIQUE TO LOCATE DAMAGE IN A BEAM USING NON- RESONANT FREQUENCY RESPONSE VIBRATION DATA

**Dr. Colin P. Ratcliffe**

Dr. Colin P. Ratcliffe
Mechanical Engineering Department
United States Naval Academy
590 Holloway Road
Annapolis, MD 21402-5002
(410) 293-6535

# A Technique to Locate Damage in a Beam Using Non-Resonant Frequency Response Vibration Data

EW-TR-07-97

Dr. Colin P. Ratcliffe
Mechanical Engineering Department
United States Naval Academy
590 Holloway Road
Annapolis
Maryland 21402

(410) 293-6535

Short Running Headline:
DAMAGE LOCATION WITH NON-RESONANT DATA

Total number of pages (including this one): 25

## ABSTRACT[1]

This paper investigates a vibrational technique for the non destructive identification of damage in beams. There has been much work investigating the variation of natural frequencies with damage, but much less on the effect of damage on mode shapes. Very little attention has been directed to off-resonant performance. This paper develops a technique for identifying the location of structural damage in a beam using experimental frequency response function data. The procedure specifically has no requirement for knowledge about the undamaged structure. Although the technique is based on modal superposition, a modal analysis of the measured data is not required, and offers no additional information.

The procedure is initially developed using a finite element model. However, the major demonstration in this paper concerns the analysis of experimental data taken from a steel beam. This was damaged with an increasingly deep, 2.8 mm wide slot. It is shown that the technique is highly sensitive, and can locate minor damage. For example, the procedure correctly located the slot when it was only 0.05 mm deep (0.8% reduction in thickness). While traditionally the onset of damage is often indicated by a change in natural frequencies, at this small level of damage the change in natural frequencies is within the bounds of experimental error, and could not be used. Other previously reported damage detection procedures were not successful at locating the slot until it was more than 2.25 mm deep.

[1]This Technical Report includes a complete family of graphs and diagrams, some of which are referenced out of order, and some of which are not mentioned at all in the text. References are in an unconventional format to aid preparation of other papers, and again, not all are mentioned in the text.

# 1. INTRODUCTION

Vibration measurements have been used for many years to identify damage in a structure. Some of the simplest techniques monitor the vibration of running equipment (for example, aircraft engines), and if the level exceeds a prescribed quantity or condition, the monitoring system sets an alarm or automatically shuts down the faulty equipment. Most of these "engine health" techniques are limited in that they cannot identify the location of the damage, only that damage exists. Increasingly, it is becoming possible to use vibration techniques to locate the damage within a structure.

Much of the previously reported work uses modal analysis to locate damage in trusses and frameworks. This work was brought about by the need to locate damage in difficult-to-reach structures such as the underwater part of offshore oil platforms, and space structures such as satellites and the space station. In these structures the change in natural frequencies caused by the failure of a single member can be large enough to be detected and used to identify damage. Many damage detection techniques, including [{Raa-{Raq], essentially treat the frames as discrete systems, and use different methods of comparing modal behavior between the undamaged and damaged states.

Compared to trusses and space frames, there is much less reported work on beams and plates. The main focus of this work is often on composite materials and concrete structures, such as bridges. For example, Javor [{Rbb] gave international guidelines recommending that the fundamental frequency of bridges is monitored for long-term observations. Miller *et al.* [{Rbc] reported on a reinforced concrete bridge, and compared experimental and finite element results to identify damage to the shoulders of the bridge using differences in natural frequencies, and anomalies in mode shapes. Liang *et al* [{Rbw] presented an energy transfer method using natural frequency and mode shape data for detecting post-earthquake damage in bridges, and Casas and Aparicio [{Rbd] minimized a scalar performance error between footprint and measured mode shapes and natural frequencies.

The mode shapes of continuous structures change with damage, and Yuen [{Rbi] documented the change in the fundamental mode shape for a cantilever with respect to the location of damage. A displacement mode shape by itself is not a reliable indicator of damage location, and several authors have considered using strain mode shapes. Chang *et al.* [{Rbk] investigated the sensitivity of modal parameters to damage and compared strain measured mode shapes with displacement mode shapes. They concluded that strain shapes were more effective at identifying the location of damage than displacement shapes. This finding is consistent with a study by Pandey *et al.* [{Rbl]. Curvature is proportional to the surface strain, and Pandey showed that the difference between the curvature mode shapes for an intact and damaged beam could locate a localized change in elastic modulus of about 30%.

The relative sensitivity of strain shapes to damage has lead to a variety of strain energy based techniques, including [{Rbq, {Rbu]. Damage is generally located by comparing some strain energy parameter with the same quantity for the structure in an undamaged state. Varying degrees of success and sensitivity are reported. When an undamaged structure is not available for analysis (or by preference for some researchers), a validated finite element model of the undamaged structure is often used as a "footprint". However, requiring this footprint can limit the application of these techniques. A study by Ratcliffe [{Rbq] introduced a technique whereby the strain mode shapes were calculated from resonant displacement mode shapes. These were then processed to yield a "Difference Function" that located the damage. Data from an undamaged structure were specifically not required.

One of the limitations of all experimental modal-based techniques is their sensitivity to data and curve fit errors. Depending on the test technique and the algorithms and curve fits used for the modal analysis, there can be an unexpectedly large errors in the modal constants. Variations in the structure itself during testing can also adversely effect the modal data, and surprisingly there is little attention to these errors in the literature [{Rbx]. The errors in modal constants are particular significant since many of the techniques rely on the differences between the constants.

The technique presented here analyzes unprocessed frequency response data, including the off-resonant data, and thus eliminates all errors associated with a modal analysis. The procedure of [{Rbv] is applied at each frequency in the spectra, and a contour plot of a Damage Index versus beam position gives a strong visual indication of the location of the damage. The procedure is validated with experimental data captured from a steel beam. A small stiffness reduction of about 2%, caused by locally reducing the thickness of a 6 mm thick (1/4 inch) beam by 0.05 mm (2/1000 inch), gave virtually no measurable change in natural frequencies. The technique presented here successfully located this small amount of damage. Other techniques presented in the literature did not locate the damage until the thickness reduction was about ??%.

## 2. STRAIN MODE SHAPES

Strain mode shapes are more sensitive indicators of damage location than displacement mode shapes, but compared to displacement shapes, they are often more difficult to measure directly. Assuming pure bending the surface strain for a beam can be related to the radius of curvature, $R$:

$$\epsilon = \frac{t}{2R} \tag{1}$$

Especially for off-resonant conditions, the displacements are small and the radius of curvature can be approximated by:

$$R = \left| \frac{\left(1 + \left(\frac{dv}{dx}\right)^2\right)^{3/2}}{\left(\frac{d^2v}{dx^2}\right)} \right| \approx \left| \frac{1}{\left(\frac{d^2v}{dx^2}\right)} \right| = \left| \frac{t}{2\epsilon} \right| \tag{2}$$

Experimental displacement mode shape data (and eigenvectors from a finite element analysis) are discrete in space. Considering Equation (2), the strain mode shape can be estimated using a finite difference approximation such as Laplace's Difference Equation [{Rbm]. Normally Laplace's equation is applied to problems involving two dimensions. In this case the mode shapes for a beam are one-dimensional, and at each resonance the Laplacian $\mathcal{L}_i$, of the discrete mode shape, $a_i$, is calculated using Laplace's Equation as:

$$\mathcal{L}_i = (a_{i+1} + a_{i-1}) - 2a_i \tag{3}$$

In this formulation it is assumed that the grid locations are equally spaced along the beam, and that the absolute values of the Laplacian are not of interest.

## 3. DAMAGE DETECTION WITH STRAIN SHAPES

As has been shown by several authors, including [{Rbl {Rbt and {Rbv], a strain mode shape by itself can sometimes reveal the location of damage. As an example, consider a uniform beam with a localized reduction in stiffness. This is representative of crack damage, and may be analyzed by reducing the thickness of one element of the finite element model, but leaving the mass matrix unchanged [{Rai] and [{Rbl]. Here the localized percentage reduction in bending stiffness, EI, is called the percentage damage. The Laplacian calculated using Equation (3) for the first bending mode of a finite element free-free beam with 75% damage between nodes #7 and #8 is shown in Figure 1. This level of damage is severe, and is easily located. With less severe damage the Laplacian retains its characteristic shape, but the effect is less pronounced. This is shown, for 15% damage to the same beam, in Figure 2. As described in the Introduction, several techniques rely on the difference between a footprint and damaged data in order to enhance this diminishing irregularity.

## 4. MODIFYING THE STRAIN SHAPES

As the level of damage further reduces, the distinctive shape of the Laplacian continues to become less pronounced. There are several methods that can be used to enhance the irregularity in the graph, such as piecewise linearization and cubic spline. The one progressed in this paper was initially proposed in [{Rbv]. The method is to fit a cubic polynomial to the Laplacian, and determine a Damage Index calculated as the numeric difference between the cubic and Laplacian. A separate cubic is determined for each element of the Laplacian in turn, with the coefficients being determined from the data on either side of the element, but excluding the actual element. For example, when the cubic calculated for the $i^{th}$ element of the Laplacian, $\mathcal{L}_i$, at position $x_i$ along the beam, is defined as:

$$p_0 + p_1 x_i + p_2 x_i^2 + p_3 x_i^3 \tag{4}$$

The coefficients $p_0$, $p_1$, $p_2$ and $p_3$ are determined using Laplacian elements:

$$\mathcal{L}_{i-2}, \mathcal{L}_{i-1}, \mathcal{L}_{i+1}, \mathcal{L}_{i+2} \tag{5}$$

The Damage Index, $\delta_i$, is then calculated from the cubic and the Laplacian.

$$\delta_i = (p_0 + p_1 x_i + p_2 x_i^2 + p_3 x_i^3) - \mathcal{L}_i \tag{6}$$

The Damage Index for 15% damage between nodes #7 and #8 is shown in Figure 3. While the Damage Index does not identify the location of damage as accurately as the Laplacian, it is a

much more sensitive parameter, in that small amounts of damage trigger significant features in the graph. Furthermore, as is shown later in the experimental section, the procedure includes an inherent smoothing process that helps reduce the effects of measurement errors.

## 5. OPERATING MODE SHAPES

Most previous experimental work has focused on using resonant modal data. As discussed above, the modal data are influenced by a variety of errors, and since the techniques may use the differences between modal constants, the effectiveness of the damage detection procedures can be seriously degraded. The errors associated with curve fitting can be eliminated by considering operating mode shapes determined directly from raw frequency response function data. The general response of a structure subject to harmonic excitation at circular frequency $\omega$ can be determined by a linear superposition of the eigenvectors. For single-point harmonic force excitation at circular frequency $\omega$, at the $j^{th}$ coordinate, the spatial response $v_i$ at the $i^{th}$ coordinate is given by:

$$\frac{v_i}{f_j} = \sum_{r=1}^{N} \frac{A_{r,i,j}}{\left(\omega_r^2 - \omega^2 + 2i\zeta_r\omega_r\omega\right)} \tag{7}$$

where N is the number of modes included in the analysis, $A_{r,i,j}$ is the modal constant associated with the $r^{th}$ natural frequency and spatial coordinates i and j, and $\omega_r$ is the $r^{th}$ natural frequency. Viscous damping is assumed in the equation, but is not essential to this exposition. This well-known equation shows that off-resonant displacement shapes (or "operating mode shapes" as they may be called) are a superposition of the resonant mode shapes.

## 6. DETECTING DAMAGE WITH THE OPERATING MODE SHAPES

The Laplacian can now be determined for an off-resonant excitation frequency. Combining equations (3) and (7) yields the general Laplacian as a function of excitation frequency and discrete position i along the beam:

$$\begin{aligned} \mathcal{L}_i^* &= (v_{i+1} + v_{i-1}) - 2v_i \\ &= \sum_{r=1}^{N} \frac{\left(a_{r,i+1,j} + a_{r,i-1,j} - 2a_{r,i,j}\right)}{\left(\omega_r^2 - \omega^2 + 2i\zeta_r\omega_r\omega\right)} \\ &= \sum_{r=1}^{N} \frac{\mathcal{L}_{r,i}}{\left(\omega_r^2 - \omega^2 + 2i\zeta_r\omega_r\omega\right)} \end{aligned} \tag{8}$$

where $\mathcal{L}_i^*$ indicates the non-resonant Laplacian function, and $\mathcal{L}_{r,i}$ is the Laplacian calculated at resonance for the $r^{th}$ mode. This equation shows that the Laplacian, or curvature shape, for any excitation frequency is a superposition of the Laplacian functions calculated at resonance. It was shown previously that damage causes a feature in the resonant Laplacian graphs, and so a feature will also exist in Laplacian functions calculated from non-resonant data.

The damage detection procedure is therefore to measure frequency response functions for an equally-spaced mesh of test coordinates along the length of a beam. The data are captured on a digital spectrum analyzer, and have a finite number of frequency lines. At each frequency line in the spectra the Laplacian of Equation (3) is determined from the operating mode shapes defined by the unprocessed frequency response data. The modulus of the complex Laplacian is then graphed as a contour plot of frequency versus position along the beam. In order to improve visualization some form of normalization is required. The most effective procedure is to normalize the Laplacian at each frequency such that the root mean square value is one.

At each frequency the complex Damage Index of Equations (4)-(6) is determined from the Laplacians, and its modulus is normalized and graphed as a contour plot.

Inspection of the contour plots can reveal a number of different conditions. Remembering that damage is located at a specific position on the beam, and that the location of the damage is independent of frequency, trends on the contour plot that are parallel to the frequency axis are indicative of structural irregularities. Features that are parallel to the spatial axis only occur at one frequency, and are associated with experimental error at resonance. Features that vary with frequency show dependency on excitation, and are typically associated with antiresonances. Figure 4 shows the Laplacian calculated from experimental frequency response data taken from a steel beam with no visually obvious damage (the full experimental setup and results are described below). The figure demonstrates the effect of both resonant and antiresonant behavior.

Figure 5 shows the Damage Index calculated from the Laplacian data in Figure 4. There appears to be a structural feature at about coordinate #27 which was not identified in the Laplacian of Figure 4. This feature is coincident with one of the 1/4-inch suspension holes. While it is hoped that the algorithm has detected the hole, the claim has not been investigated fully, and is not made in this paper. Features on the contour plots are best observed when the plots are in color. In the reduction to monochrome, the lowest valued contour was erased. All peaks above an arbitrary contour at about RMS=0.35 were flood-filled with black. Also, plotting the square of the modulus generally produced an image more amenable to monochromatic rendition, and is the procedure used for the figures shown here.

## 7. EXPERIMENTAL DEMONSTRATION

### 7.1 EXPERIMENTAL CONFIGURATION

A flat steel beam, 0.9 m × 0.075 m × 6.3 mm thick (36 inch × 3 inch × 0.249 inch), was suspended through two 6 mm holes positioned 1/4 and 3/4 down the length, and centered 12 mm from one edge of the beam. Suspension was with monofilament and rubber bungee cords. A uniform mesh of test coordinates was placed on the beam as shown in Figure 6. The beam was initially tested by measuring frequency response functions between each test coordinate and an accelerometer fixed at coordinate #1 (centerline, left end). Modal data are not required for the damage detection procedure, however for visualization and to assess data quality, the data were subject to a modal analysis using the commercial STAR software. For the frequency range tested (0-1.5 kHz), 13 natural frequencies were identified, there being eight 'bending' and five 'torsional' modes. Viscous damping was typically 0.1-0.5%.

The beam was then damaged with an increasingly deep 2.8 mm (7/64 inch) wide groove milled across the width of one face of the beam and centered 0.33 m (13 inch) from one end. The width of the groove was kept as small as possible, commensurate with being able to use a depth gage to measure its depth. The groove introduced a stiffness change, with minimal effect on the mass of the beam. The beam was tested with a total of ?? different groove depths, ranging from 2/1000 inch to ??. At each groove depth the frequency response function data collection for the 72 coordinate locations and the modal analysis were repeated. For comparison only the percentage change in experimental natural frequencies for the first four bending modes are shown in Figure 7.

### 7.2 EXPERIMENTAL RESULTS

For all the contour plots, the "Beam Position" is the grid number. There were 36 grids, starting 0.5 inch from one end, with the last grid being 35.5 inch from that end. The groove is marked on the plots as a straight line mid way between grids #12 and #13. The "Frequency Index" on the plots is the number of the frequency line in each spectrum. Lines 50-700 from 801-line 0-1.56 kHz spectra were used, thus the actual frequency is calculated as (frequency index +49)×1560/800 Hz.

Figure 9 shows the Damage Index for a groove depth of 0.002 inch. Even at this very low level of damage (0.8% reduction in thickness) the Damage Index shows a trend (an area of black parallel to the frequency axis) near beam position 12-13. This is coincidental with the actual location of the damage. This feature in the Damage Index contour plot becomes further enhanced as the groove is made deeper into the beam. Depths of 0.005 inch or greater cause the dominant feature on the Damage Index plot to correctly identify the damage location without ambiguity. Damage Indices for 0.005 inch and 0.030 inch depths are shown in Figures 13 and 23.

Other previously published damage location procedures discussed above considered modal data, and inspect either the curvature or the change in curvature caused by the damage. With this experiment, curvature shapes did not give any indication of damage until the groove depth was 90/1000 inch (36% reduction in thickness, 74% localized stiffness reduction). The curvature shape with this condition for mode 1 is shown in Figure 38. The difference in curvature between a damaged and undamaged structure never successfully located the damage. The difference in curvature for the maximum groove depth of 110/1000 inch (44% reduction in thickness, 83% localized stiffness reduction) for mode 1 is shown in Figure 45. Figure 43 shows the difference in curvature plotted as a contour plot for all frequencies. Generous interpretation may indicate a feature close to the groove (beam position 12.5), but this is not sufficiently marked to warrant a claim of damage. The reason for the apparent failure of the curvature difference method was not investigated. For comparison, the Damage Index for the 110/1000 inch deep groove is shown in Figure 42.

## 8. DISCUSSION AND CONCLUSIONS

This paper has presented a sensitive technique that uses non-resonant frequency response data to locate damage in an otherwise uniform beam. The procedure consists of converting displacement data to strain mode shapes by applying a discrete finite difference approximation. The resulting strain shapes are further processed to reveal the location of damage. The procedure is applied separately at each frequency in the frequency response functions, and presented as a contour plot of $(\text{modulus})^2$. Features on the contour plot which appear for one beam location, but at many frequencies, represent structural irregularities. The procedure correctly located a very small quantity of damage, 2/1000 inch in a 250/1000 inch thick beam.

Previous work by several authors considered locating the damage using the difference in curvature of a beam before and after damage. Curvature shapes for the fundamental mode located the damage once the depth was 90/1000 inch (about one-third of the depth). Resonant Difference in curvature procedures did not locate the damage at the maximum groove depth of 110/1000 inch.

REFERENCES

{Raa. R. D. Begg and A. C. Mackenzie 1978 *Proceedings of IES Symposium - Integrity of Offshore Structures.* Monitoring of offshore structures using vibration analysis.

{Rab. O. Loland and C. J. Dodds 1976 *Proceedings of the 8th Annual Offshore Technology Conference* Paper No. 2551, **2**, 313-319. Experiences in developing and operating integrity monitoring systems in North Sea.

{Rac. J. K. Vandiver 1975 *Proceedings of the 7th Annual Offshore Technology Conference* Paper No. 2267, **2**, 243-252. Detection of structural failure on fixed platforms by measurements of dynamic response.

{Rad. T. A. L. Kashangaki 1995 *AIAA/ASME/ASCE/AHS Structures, Structural Dynamics & Materials Conference* Collection of Technical Papers **3**, 1535-1542. Mode selection for damage detection using the modal sensitivity parameter.

{Rae. S. Rubin 1980 *Journal of the Engineering Mechanics Division, EM3,* 425-441. Ambient vibration survey of offshore platform.

{Raf. P. Hajela and F. J. Soeiro 1990 *American Institute of Aeronautics and Astronautics Journal* **28**(6), 1110-1115. Structural damage detection based on static and modal analysis.

{Rag. L. B. Crema A. Castellani and G. Coppotelli 1995 *Materials and Design Technology American Society of Mechanical Engineers, Petroleum Division* Publication PD v71. Damage localization in composite material structures by using eigenvalue measurements.

{Rah. P. Cawley and R. D. Adams 1979 *Journal of Composite Materials* **13**, 161-175. A vibration technique for non-destructive testing of fibre composite structures.

{Rai. P. Cawley and R. D. Adams 1979 *Journal of Strain Analysis* **14**(2), 49-57. The location of defects in structures from measurements of natural frequencies.

{Raj. P. Cawley and R. D. Adams 1980 *Proceedings of the Third International Conference on Composite Materials* 973-983. Defect location in structures made from advanced composite materials.

{Rak. R. A. Manning 1994 *American Institute of Aeronautics and Astronautics Journal* **32**(6) Technical Notes, 1331-3. Structural damage detection using active members and neural networks.

{Ral. P. L. Liu 1995 *Journal of Structural Engineering* **121**(4), 599-607. Identification and damage detection of trusses using modal data.

{Ram. J. C. Chen and J. A. Garba 1988 *American Institute of Aeronautics and Astronautics Journal* **26**(9), 1119-1126. On-orbit damage assessment for large space structures.

{Ran. C. Li and S. W. Smith 1995 *Journal of Guidance, Control, and Dynamics* **18**(3), 419-425. Hybrid approach for damage detection in flexible structures.

{Rao. R. D. Adams, J. M. W. Brownjohn and P. Cawley 1991 *Non Destructive Testing and Examination International Journal* **24**(3), 123-134. Detection of defects in GRP lattice structures by vibration measurements.

{Rap. T. W. Lim and T. A. L. Kashangaki 1994 *American Institute of Aeronautics and Astronautics Journal* **32**(5), 1049-1057. Structural damage detection of space truss structures using best achievable eigenvectors.

{Raq. F. Shahrivar and J. G. Bouwkamp 1986 *Journal of Energy Resources Technology* **108**, 97-106. Damage detection in offshore platforms using vibration information.

{Rar. I. Peroni A. Paolozzi and A. Bramante 1991 *Proceedings of the 9th International Modal Analysis Conference* **2**, 1617-1622. Effect of debonding damage on the modal damping of a sandwich panel.

{Ras. J. Y. Lai and K. F. Young 1995 *Journal of Composite Structures* **30**(1), 25-32. Dynamics of graphite/epoxy composite under delamination fracture and environmental effects.

{Rat. J. Vantomme 1992 *Journal of Composite Structures* **22**(4), 201-205 Evaluation of structural joints in composites with modal parameters.

{Rau. C. S. Lin 1990 *American Institute of Aeronautics and Astronautics Journal* **28**, 1650-1654. Location of modeling errors using modal test data.

{Rav. Y. S. Park, H. S. Park and S. S. Lee 1988 *International Journal of Analytical and Experimental Modal Analysis* **3**(3), 101-107. Weighted-error-matrix application to detect stiffness damage by dynamic characteristic measurement.

{Raw. M. A. Mannan and M. H. Richardson 1990 *Proceedings of the 8th International Modal Analysis Conference* **1**, 652-657. Detection and location of structural cracks using FRF measurements.

{Rax. H. P. Gysin 1986 *Proceedings of the 4th International Modal Analysis Conference* **2**, 1339-1351. Critical application of the error matrix method for localization of finite element modeling inaccuracies.

{Ray. H. M. Kim and T. J. Bartkowicz 1995 *Sound and Vibration* April. Health monitoring of large structures.

{Raz. G. Hearn and R. B. Testa 1991 *Journal of Structural Engineering* **117**(10) Modal analysis for damage detection in structures.

{Rba. A. K. Pandey and M. Biswas 1994 *Journal of Sound and Vibration* **169**(1), 3-17. Damage detection in structures using changes in flexibility.

{Rbb. T. Javor 1991 *Journal of Materials and Structures* **142**, 253-259. Damage classification of concrete structures; the state of the art report of RILEM Technical Committee 104-DCC activity.

{Rbc. R. A. Miller, A. E. Aktan and B. M. Shahrooz 1992 *American Society of Civil Engineers* Nondestructive Testing of Concrete Elements and Structures 150-161. Nondestructive and destructive testing of a three span skewed R.C. slab bridge.

{Rbd. J. R. Casas and A. C. Aparicio 1994 *Journal of Structural Engineering* **120**(8). Structural damage identification from dynamic-test data.

{Rbe. A. C. Okafor, K. Chandrashekhara and Y. P. Jiang 1995 *Smart Structures and Materials: Smart Sensing, Processing, and Instrumentation, Proceedings of SPIE -The International Society for Optical Engineering* **2444**, 314-325. Damage detection in composite laminates with built-in piezoelectric devices using modal analysis and neural network.

{Rbf. P. F. Rizos, N. Aspragathos and A. D. Dimarogonas 1990 *Journal of Sound and Vibration* **138**, 381-388. Identification of crack location and magnitude in a cantilever beam from the vibration modes.

{Rbg. W. T. Springer, K. L. Lawrence and T. J. Lawley 1988 *Experimental Mechanics* **28**, 34-37. Damage assessment based on the structural frequency-response function.

{Rbh. J. F. Doyle 1995 *Experimental Mechanics* **35**(3), 272-280. Determining the size and location of transverse cracks in beams.

{Rbi. M. M. F. Yuen 1995 *Journal of Sound and Vibration* **103**, 301-310. A numerical study of the eigenparameters of a damaged cantilever.

{Rbj. G. C. Yao, K. C. Chang and G. C. Lee 1992 *Journal of Engineering Mechanics* **118**,(9) Damage diagnosis of steel frames using vibrational signature analysis.

{Rbk. K. C. Chang, Z. Shen and G. C. Lee 1993 *American Society of Civil Engineers Proceedings of the Symposium of Structural Engineering, Natural Hazards and Mitigation* 1083-1088. Modal analysis technique for bridge damage detection.

{Rbl. A. K. Pandey, M. Biswas and M. M. Samman 1991 *Journal of Sound and Vibration* **145**(2), 321-332. Damage detection from changes in curvature mode shapes.

{Rbm. S. C. Chapra and R. P. Canale 1988 McGraw Hill Numerical methods for engineers, 2nd Edition.

{Rbn. O. Bernasconi and D. J. Ewins 1989 *Proceedings of the 7th International Modal Analysis Conference* **2**, 1453-1464. Application of strain modal testing to real structures.

{Rbo. D. B. Li, H. C. Zhuge and B. Wang 1989 *Proceedings of the 7th International Modal Analysis Conference* **2**, 1285-1289. The principles and techniques of experimental strain modal analysis.

{Rbp. W. F. Tsang 1990 *Proceedings of the 8th International Modal Analysis Conference* **2**, 1246-1251. Use of dynamic strain measurements for the modeling of structures.

{Rbq. S. H. Petro, S. C. Chen, H. V. S. GangaRao and S. Venkatappa 1997 *Proceedings of the 15th International Modal Analysis Conference* **1**, 113-117. Damage Detection using Vibration Measurements.

Armored Vehicle Launched Bridge - modal analysis, "strain energy damage index" comparing damaged to undamaged.

{Rbr. M. M. Samman. 1997 *Proceedings of the 15th International Modal Analysis Conference* **1**, 627-630. Structural Damage Detection using the Modal Correlation Coefficient (MCC).

Variation of MAC, compares damaged to undamaged.

{Rbs. E. J. Williams, A. Messina and B. S. Payne. 1997 *Proceedings of the 15th International Modal Analysis Conference* **1**, 652-657. A Frequency-Change Correlation Approach to Damage Detection.

Tracks several nat freqs, and change is used to locate damage.

{Rbt. N. M. M. Maia, J. M. M. Silva and R. P. C. Sampaio. 1997 *Proceedings of the 15th International Modal Analysis Conference* **1**, 942-946. Localization of Damage using Curvature of the Frequency-Response-Functions.

Uses raw FRF, but still compares damaged to undamaged. Further process Laplacian by differentiating to enhance irregularity.

{Rbu. P. Cornwell, S. W. Doebling and C. R. Farrar. 1997 *Proceedings of the 15th International Modal Analysis Conference* **2**, 1312-1318. Application of the Strain Energy Damage Detection Method to Plate-Like Structures.

FARRAR - FE analysis had moderate success. Used plate strain-energy relationships.

{Rbv. C. P. Ratcliffe. 1997 *Journal of Sound and Vibration* **???**(?), ???-???. Damage detection using a modified Laplacian operator on mode shape data.

{Rbw. Z. Liang, G. C. Lee and F. Kong. 1997 *Proceedings of the 15th International Modal Analysis Conference* **1**, 308-312. On detection of damage location of bridges.

{Rbx. C. R. Farrar, S. W. Doebling, P. J. Cornwell, E. G. Straser. 1997 *Proceedings of the 15th International Modal Analysis Conference* **1**, 257-263. Variability of modal parameters measured on the Alomosa Canyon bridge.

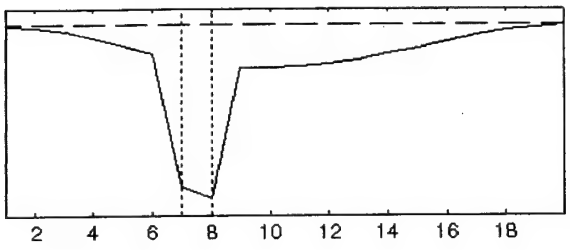


Figure 1: Laplacian for 50% damage.

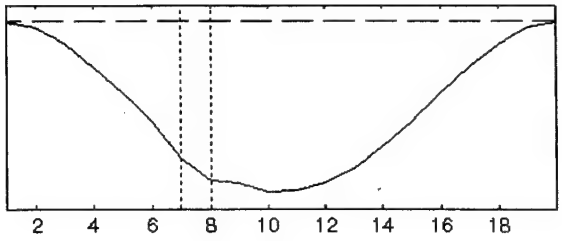


Figure 2: Laplacian for 5% damage.

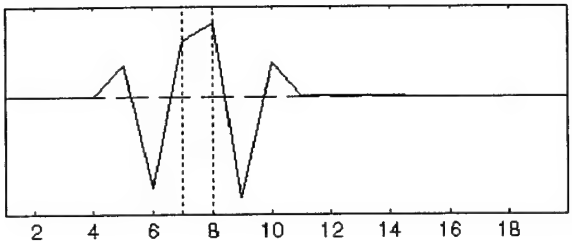


Figure 3: Damage Index for 5% damage (free-free).

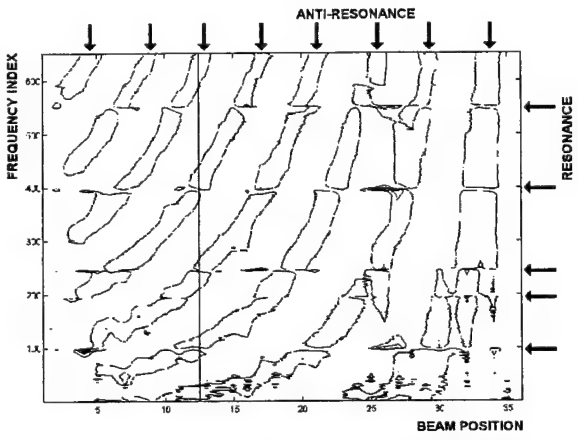


Figure 4: Laplacian undamaged beam

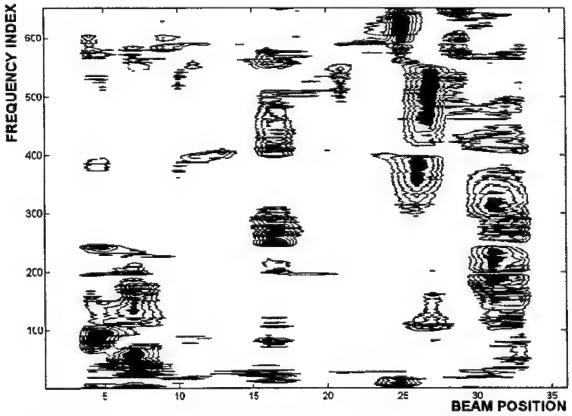


Figure 5: Damage Index undamaged beam

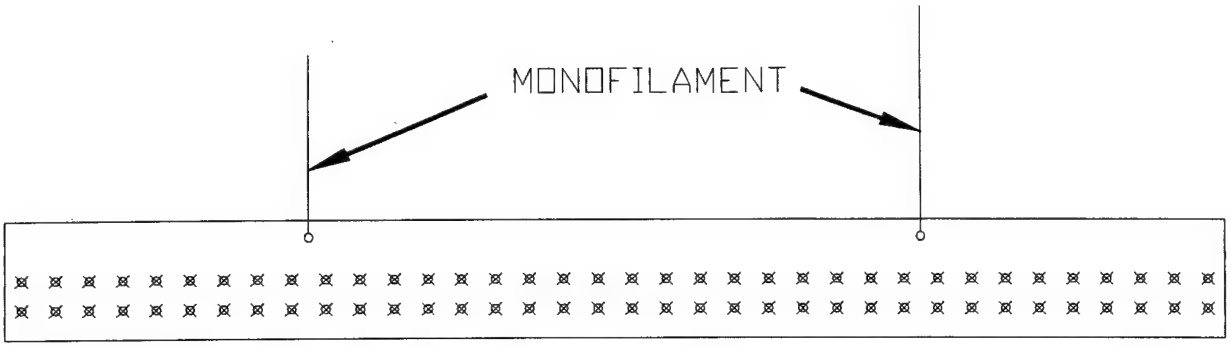


Figure 6: Mesh of test coordinates.

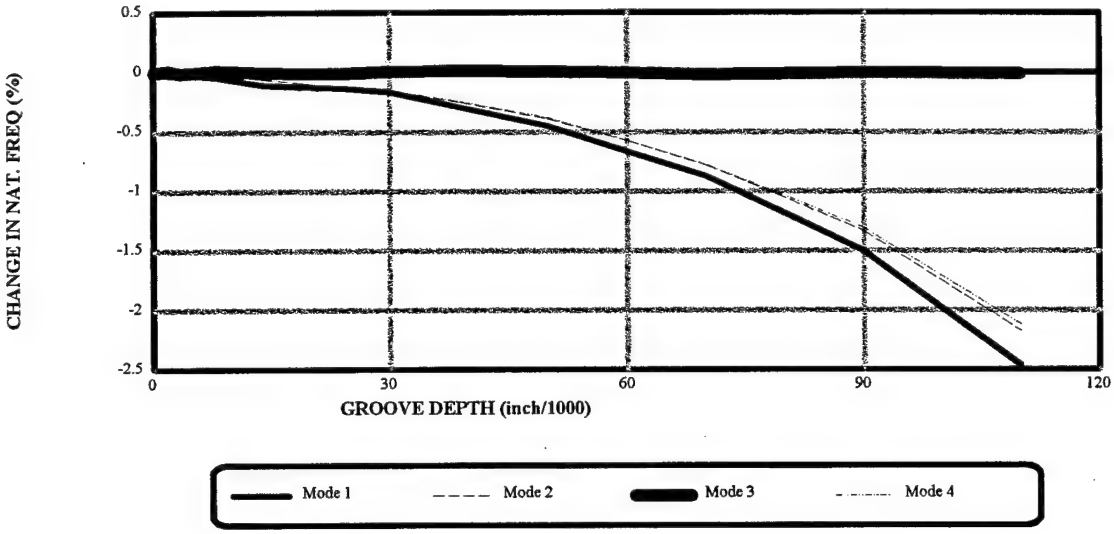


Figure 7: Change in experimental natural frequencies.

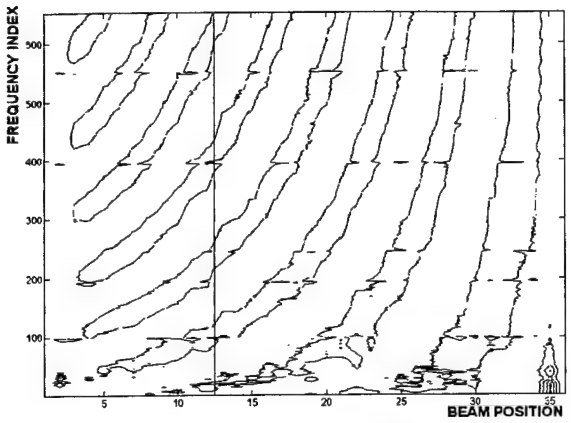


Figure 8: Laplacian 2/1000 inch

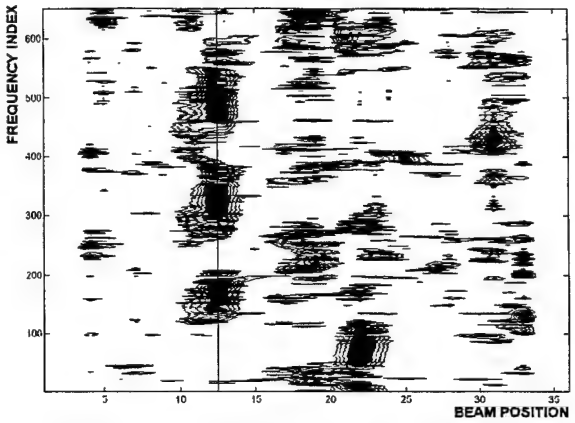


Figure 9: Damage Index 2/1000 inch

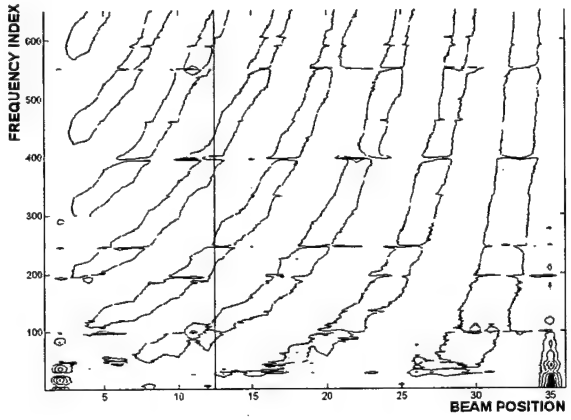


Figure 10: Laplacian 3.5/1000 inch

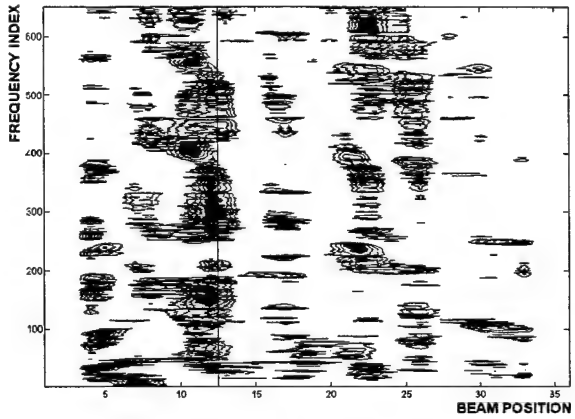


Figure 11:Damage Index 3.5/1000 inch

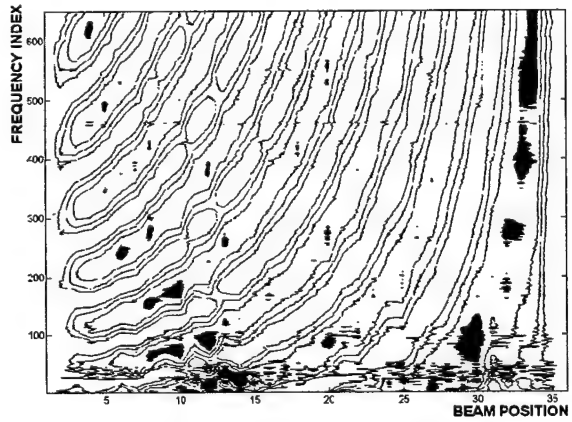


Figure 12: Laplacian 5/1000 inch

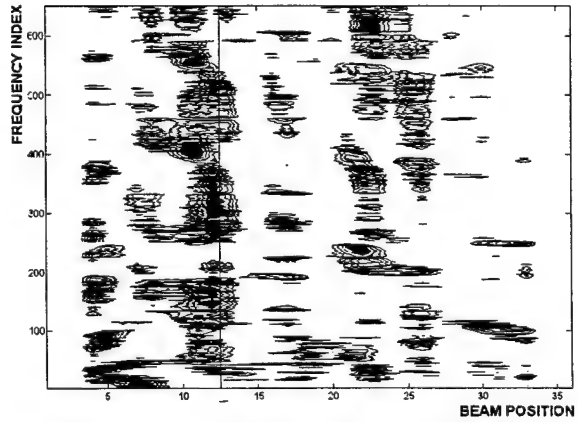


Figure 13: Damage Index 5/1000 inch

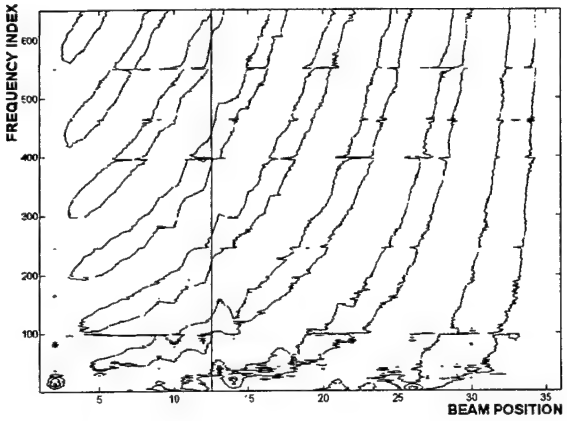


Figure 14: Laplacian 8/1000 inch

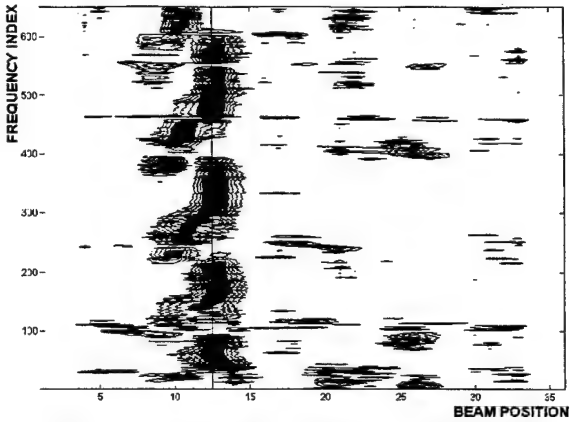


Figure 15: Damage Index 8/1000 inch

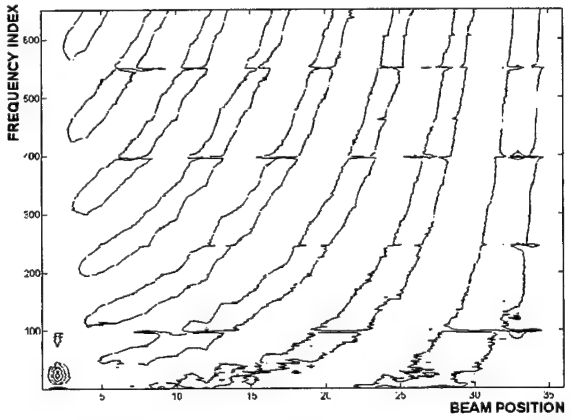


Figure 16: Laplacian 14/1000 inch

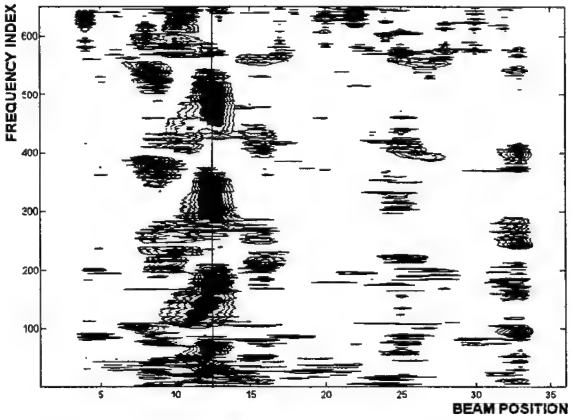


Figure 17: Damage Index 14/1000 inch

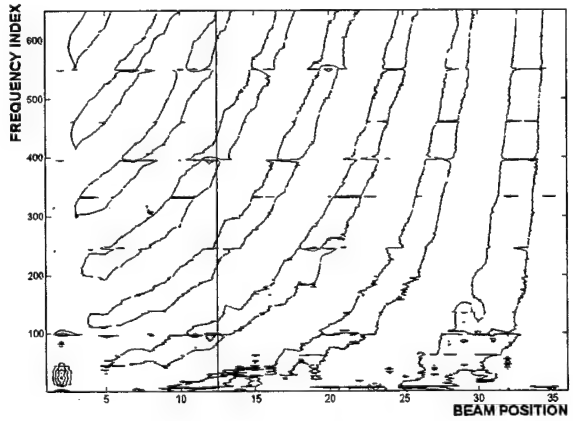


Figure 18: Laplacian 19/1000 inch

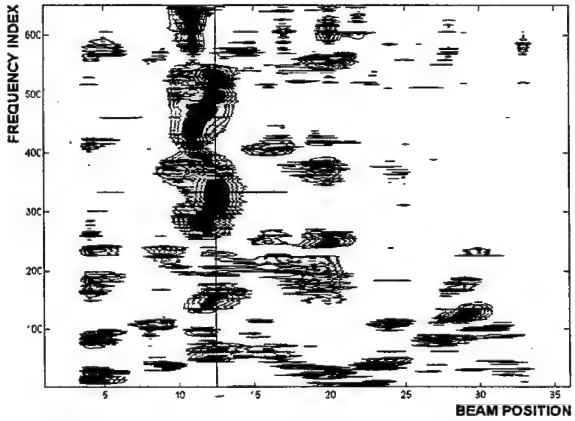


Figure 19: Damage Index 19/1000 inch

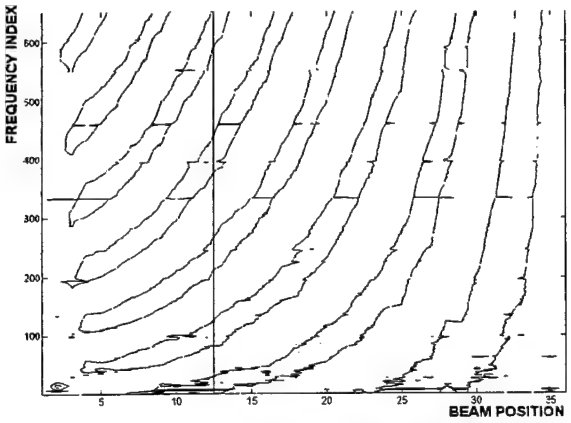


Figure 20: Laplacian 24/1000 inch

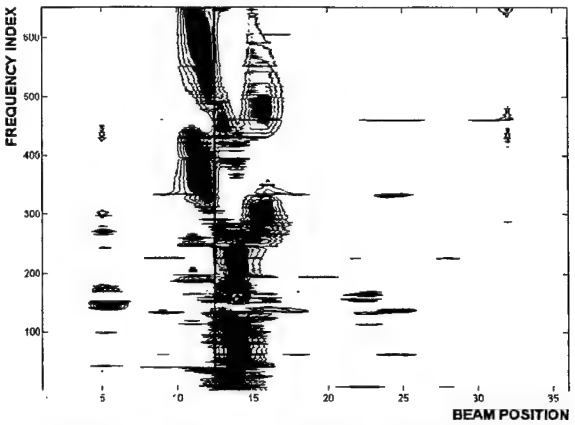


Figure 21: Damage Index 24/1000 inch

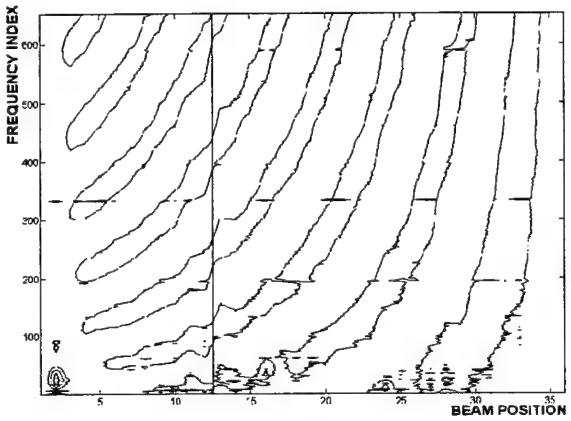


Figure 22: Laplacian 30/1000 inch

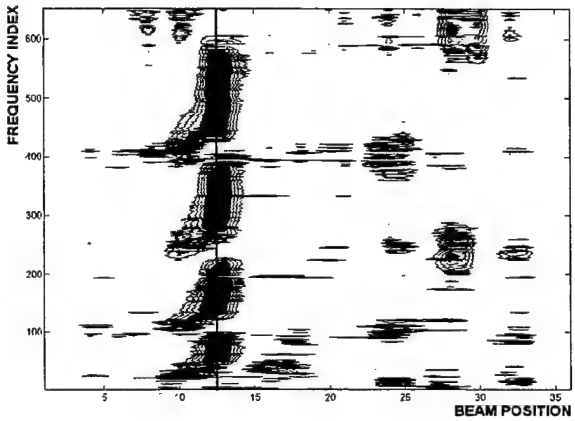


Figure 23: Damage Index 30/1000 inch

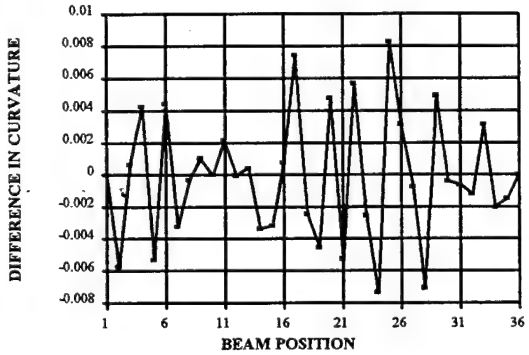


Figure 24: Difference in Curvature for 30/1000 inch, Mode 1.

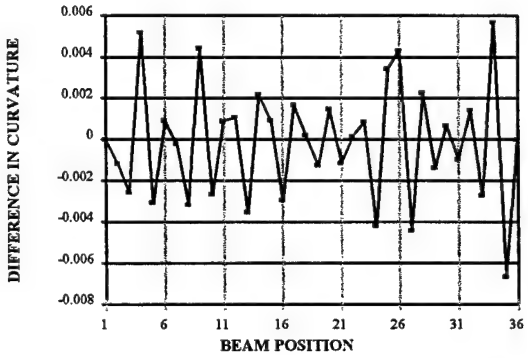


Figure 25: Difference in Curvature for 30/1000 inch, Mode 2.

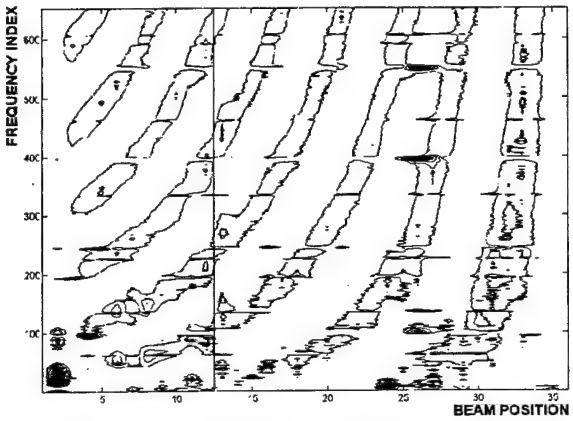


Figure 26: Laplacian difference 30/1000 inch

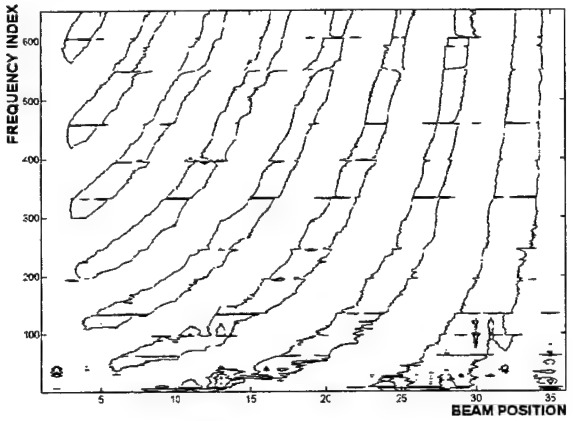


Figure 27: Laplacian 39/1000 inch

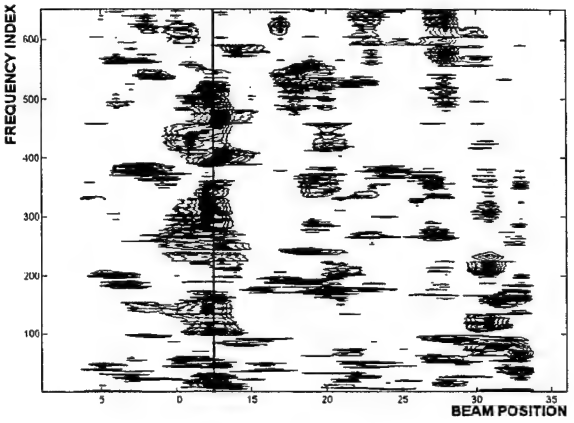


Figure 28: Damage Index 39/1000 inch

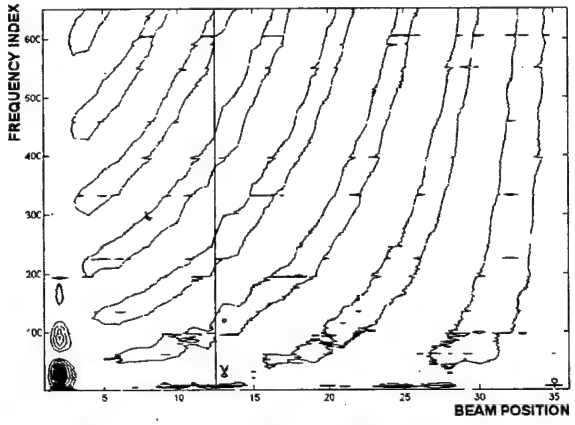


Figure 29: Laplacian 50/1000 inch

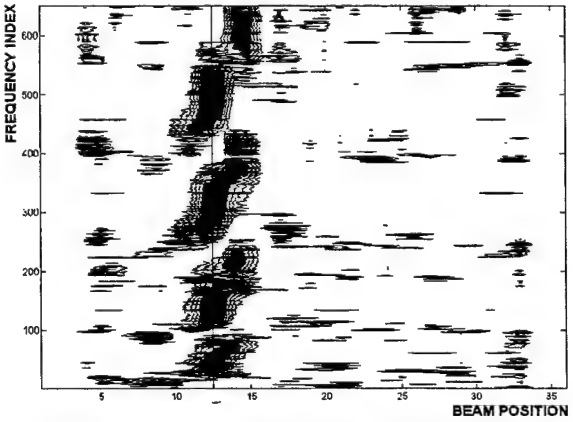


Figure 30: Damage Index 50/1000 inch

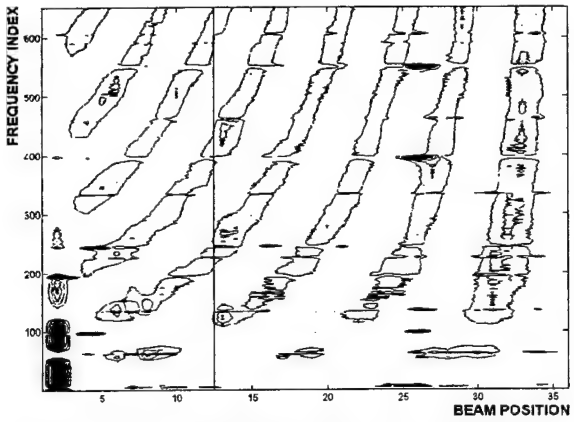


Figure 31: Laplacian difference 50/1000 inch

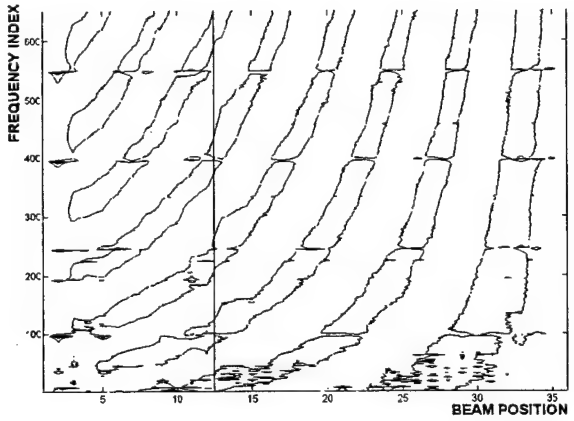


Figure 32: Laplacian 60/1000 inch

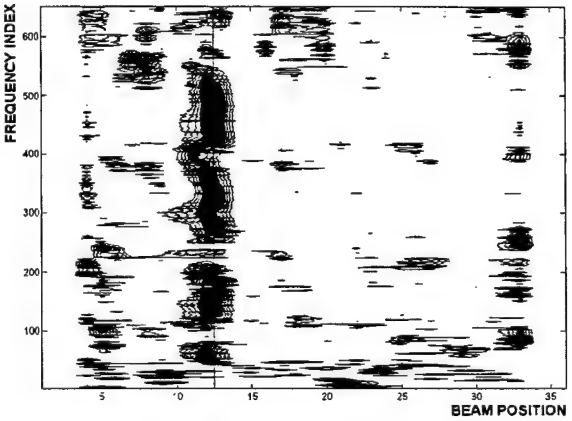


Figure 33: Damage Index 60/1000 inch

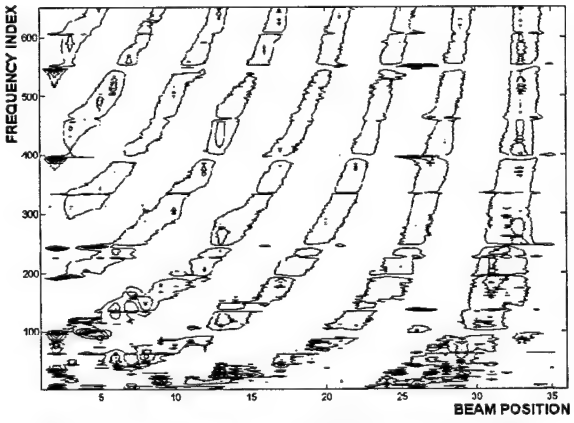


Figure 34: Laplacian difference 60/1000 inch

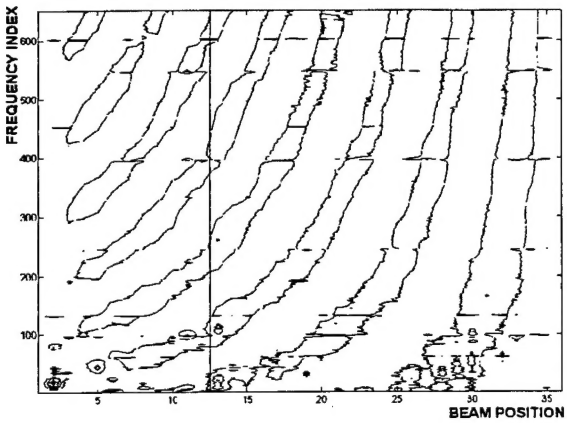


Figure 35: Laplacian 90/1000 inch

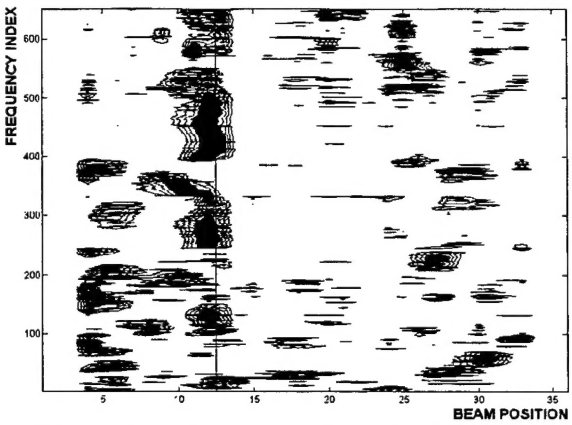


Figure 36: Damage Index 90/1000 inch

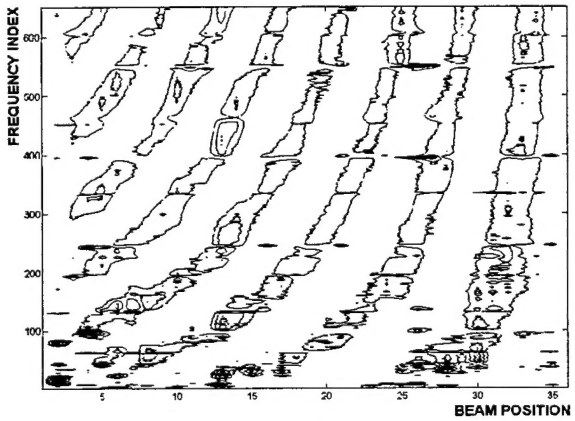


Figure 37: Laplacian difference 90/1000 inch

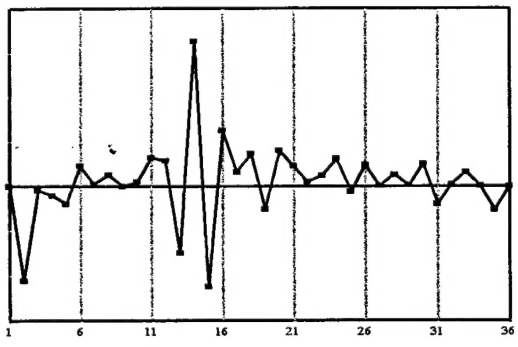

Figure 38: Laplacian for mode 1, 90/1000 inch

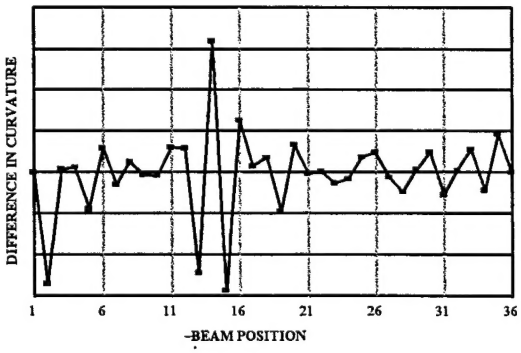


Figure 39: Difference in curvature for mode 1, 90/1000 inch

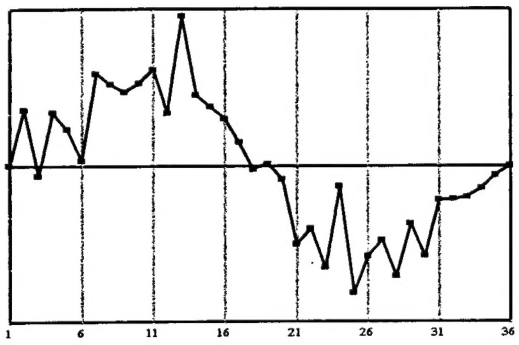


Figure 40: Laplacian for mode 2, 90/1000 inch

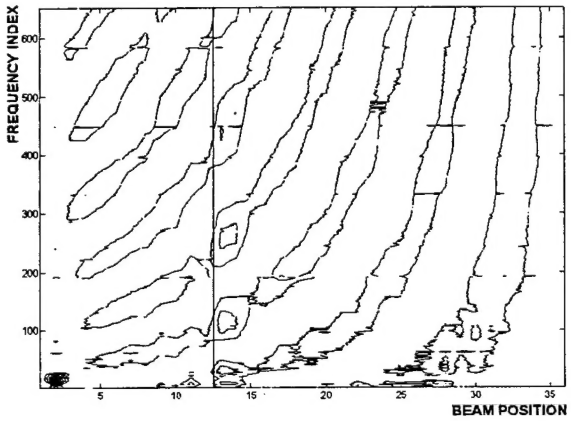


Figure 41: Laplacian 110/1000 inch

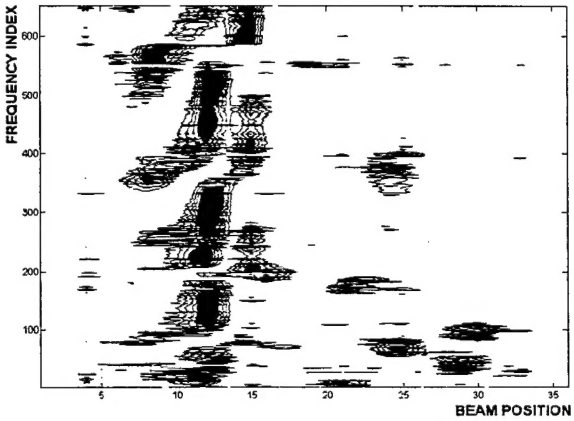


Figure 42: Damage Index 110/1000 inch

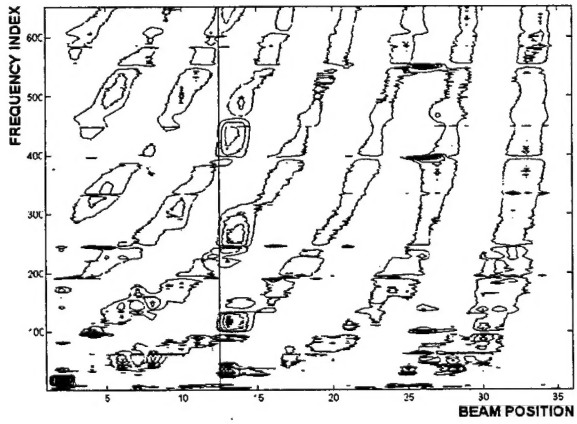


Figure 43: Laplacian difference 110/1000 inch

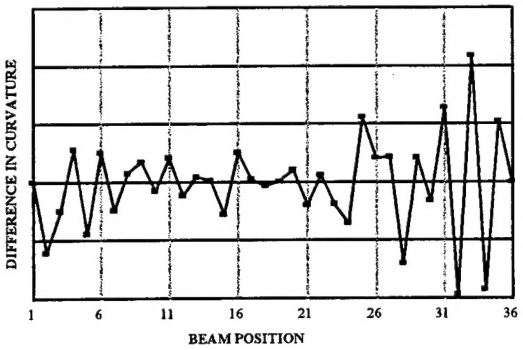


Figure 45: Curvature difference mode 1 110/1000 inch

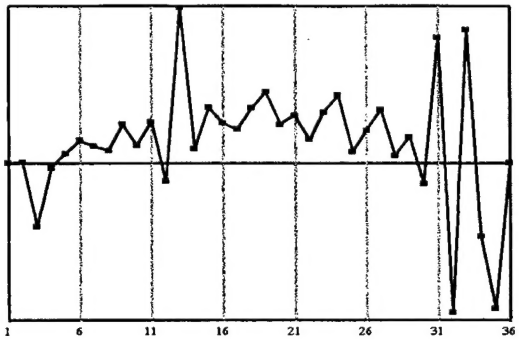


Figure 44: Laplacian Mode 1 110/1000 inch

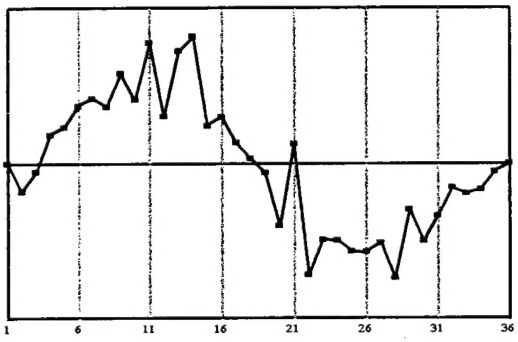


Figure 46: Laplacian Mode 2 110/1000 inch

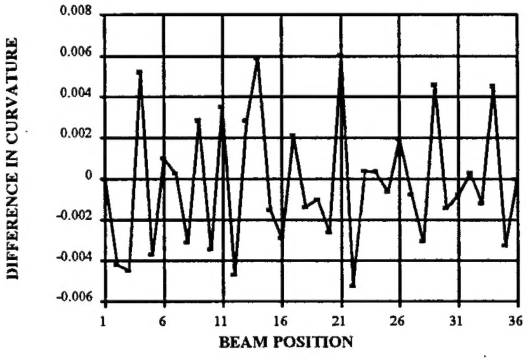


Figure 47: Curvature difference mode 2 110/1000 inch

## PLEASE CHECK THE APPROPRIATE BLOCK BELOW:

-AQ # _____

☐ _____ copies are being forwarded. Indicate whether Statement A, B, C, D, E, F, or X applies.

☑ DISTRIBUTION STATEMENT A:
APPROVED FOR PUBLIC RELEASE: DISTRIBUTION IS UNLIMITED

☐ DISTRIBUTION STATEMENT B:
DISTRIBUTION AUTHORIZED TO U.S. GOVERNMENT AGENCIES ONLY; (Indicate Reason and Date). OTHER REQUESTS FOR THIS DOCUMENT SHALL BE REFERRED TO (Indicate Controlling DoD Office).

☐ DISTRIBUTION STATEMENT C:
DISTRIBUTION AUTHORIZED TO U.S. GOVERNMENT AGENCIES AND THEIR CONTRACTORS; (Indicate Reason and Date). OTHER REQUESTS FOR THIS DOCUMENT SHALL BE REFERRED TO (Indicate Controlling DoD Office).

☐ DISTRIBUTION STATEMENT D:
DISTRIBUTION AUTHORIZED TO DoD AND U.S. DoD CONTRACTORS ONLY; (Indicate Reason and Date). OTHER REQUESTS SHALL BE REFERRED TO (Indicate Controlling DoD Office).

☐ DISTRIBUTION STATEMENT E:
DISTRIBUTION AUTHORIZED TO DoD COMPONENTS ONLY; (Indicate Reason and Date). OTHER REQUESTS SHALL BE REFERRED TO (Indicate Controlling DoD Office).

☐ DISTRIBUTION STATEMENT F:
FURTHER DISSEMINATION ONLY AS DIRECTED BY (Indicate Controlling DoD Office and Date) or HIGHER DoD AUTHORITY.

☐ DISTRIBUTION STATEMENT X:
DISTRIBUTION AUTHORIZED TO U.S. GOVERNMENT AGENCIES AND PRIVATE INDIVIDUALS OR ENTERPRISES ELIGIBLE TO OBTAIN EXPORT-CONTROLLED TECHNICAL DATA IN ACCORDANCE WITH DoD DIRECTIVE 5230.25, WITHHOLDING OF UNCLASSIFIED TECHNICAL DATA FROM PUBLIC DISCLOSURE, 6 Nov 1984 (Indicate date of determination). CONTROLLING DoD OFFICE IS (Indicate Controlling DoD Office).

☐ This document was previously forwarded to DTIC on _____ (date) and the AD number is _____.

☐ In accordance with provisions of DoD instructions, the document requested is not supplied because:

☐ It will be published at a later date. (Enter approximate date, if known).

☐ Other. (Give Reason)

**DoD Directive 5230.24, "Distribution Statements on Technical Documents," 18 Mar 87, contains seven distribution statements, as described briefly above. Technical Documents must be assigned distribution statements.**

Lawrence E. Clemens
**Print or Type Name**

410-293-6926
**Telephone Number**

**Authorized Signature/Date**

TOTAL P.02